A simulation model of organic matter and nutrient accumulation in mangrove wetland soils

RONGHUA CHEN & ROBERT R. TWILLEY*
Department of Biology, University of Southwestern Louisiana, Lafayette, Louisiana
*70504-2451, USA (*Corresponding author: Fax: 318-482-5834; Phone: 318-482-6146;*
E-mail: rtwilley@usl.edu)

Abstract. The distribution and accumulation of organic matter, nitrogen (N) and phosphorus (P) in mangrove soils at four sites along the Shark River estuary of south Florida were investigated with empirical measures and a process-based model. The mangrove nutrient model (NUMAN) was developed from the SEMIDEC marsh organic matter model and parameterized with data from mangrove wetlands. The soil characteristics in the four mangrove sites varied greatly in both concentrations and profiles of soil carbon, N and P. Organic matter decreased from 82% in the upstream locations to 30% in the marine sites. Comparisons of simulated and observed results demonstrated that landscape gradients of soil characteristics along the estuary can be adequately modeled by accounting for plant production, litter decomposition and export, and allochthonous input of mineral sediments. Model sensitivity analyses suggest that root production has a more significant effect on soil composition than litter fall. Model simulations showed that the greatest change in organic matter, N, and P occurred from the soil surface to 5 cm depth. The rapid decomposition of labile organic matter was responsible for this decrease in organic matter. Simulated N mineralization rates decreased quickly with depth, which corresponded with the decrease of labile organic matter. The increase in organic matter content and decrease in soil bulk density from mangrove sites at downstream locations compared to those at upstream locations was controlled mainly by variation in allochthonous inputs of mineral matter at the mouth of the estuary, along with gradients in mangrove root production. Research on allochthonous sediment input and in situ root production of mangroves is limited compared to their significance to understanding nutrient biogeochemistry of these wetlands. More accurate simulations of temporal patterns of nutrient characteristics with depth will depend on including the effects of disturbance such as hurricanes on sediment redistribution and biomass production.

Introduction

Long-term geomorphic and geochemical processes along with primary production largely control the formation, physical properties and chemical

composition of mangrove wetland soils (Thom 1982). Soil chemical and physical characteristics have been suggested as significant constraints of mangrove structure and productivity (Boto & Wellington 1984; Twilley 1995). Furthermore soil formation has also been considered an important process contributing to biogenic carbon sinks in tropical coastal regions (Twilley et al. 1992; Parkinson et al. 1994). Soil formation in mangrove wetlands, as in other intertidal wetlands, is the combination of several ecological processes including organic matter production (above and below ground components), export, decomposition, and burial; as well as sedimentation of allochthonous inorganic matter. Organic matter dynamics are tightly coupled to the biogeochemical cycles of nitrogen (N) and phosphorus (P) in wetland soils by the processes of decomposition, mineralization and plant uptake.

Quantifying these processes can provide insights into the biogeochemistry of mangrove soils and nutrient recycling and their effects on mangrove forest development. However, the temporal scales of these soil processes in mangrove wetlands vary from daily to thousands of years (Scholl 1964a, b). Biogeochemical models that reconstruct sediment profiles can provide insights into the relative significance of these processes to the accumulation of organic matter and nutrients in wetland soils (Morris & Bowden 1986). This will provide a better understanding of how the time scales of geophysical and ecological processes control soil fertility gradients in mangrove wetlands. Results of these simulation models of nutrient biogeochemistry can then be used to link geophysical processes to forest dynamics that are simulated in similar decadal time periods (Chen & Twilley 1998).

To study nutrient biogeochemistry of mangrove soils, we developed a simulation model, NUMAN, based on published models for marsh (SEMIDEC, Morris & Bowden 1986) and grassland communities (CENTURY, Parton et al. 1987). The objectives of this study were to: (1) quantify profiles of soil organic matter, N and P concentrations with depth in mangrove soils along the Shark River estuary of the Everglades National Park; (2) modify the SEMIDEC model to examine the effects of forest production, litter export, decomposition and sedimentation on organic matter, N and P distributions in mangrove soils; (3) calibrate NUMAN with measurements of spatially explicit variables along the Shark River estuary; (4) identify key ecological processes from sensitivity analyses of NUMAN that account for spatial and temporal differences in mangrove soil constituents along the estuary. We used NUMAN to project changes in soil organic matter and nutrients in riverine forests to test the relative importance of ecological and geophysical processes on the biogeochemistry of mangroves along the Shark River estuary. The structure of these models and sensitivity analyses of

selected functions can provide important insights to the ecologically significant processes of soil formation in mangrove wetlands.

Study site

Plots were established in four mangrove sites (S1, S3, S4 and S6) and sampled for soil characteristics along the Shark River estuary in the Everglades National Park at distances about 1.8, 4.1, 9.9 and 18.2 km, respectively, from the mouth of the estuary (Chen 1996; Chen & Twilley 1998). This region consists of 1–4 m deep peat accumulating above a mainland carbonate Oolite platform (Davis 1940; Scholl 1964a, b). Mangrove habitats in S1 and S3 are referred to as downstream locations of the Shark River estuary, while S4 is intermediate and S6 is an upstream location, following the terminology of Duke (1992). Plots were about 10 to 20 m inland from the estuary at sites S1, S3 and S4, and about 5 m inland at S6 due to the restricted zone of mangroves along this upstream region. The major source of freshwater to the estuary is from the Shark River Slough, and a salinity gradient is represented by average pore water salinities of 3.6, 14.3, 17.3 and 27.5 g/kg at S6, S4, S3 and S1, respectively. Forest basal area increased along this salinity gradient from lower values in the upper and intermediate estuary (20.7 and 19.6 m^2/ha) to nearly double these values in the lower estuary (40 m^2/ha) (Chen & Twilley 1998). *Laguncularia racemosa* had a higher importance value in the lower estuary, whereas *Rhizophora mangle* dominated in the intermediate and upper estuary.

Soil chemical analyses

We report on the depth distribution of soil characteristics at four mangrove sites along the Shark River estuary using three sampling approaches described in Chen (1996). Three stations were randomly selected in each mangrove site and marked for three repeated measures of soil total nutrient and N mineralization in August 1994, January and May 1995. For total nutrient concentrations, cores with a 5.0 cm diameter were sampled to a depth of 40 cm and sectioned at 10 cm intervals. Soil subsamples were oven dried to constant weight at 60 °C and ground with a Wiley Mill to pass through a 250 μm mesh. Total C and N content of two replicates of each sample were determined with a LECO elemental analyzer using standard protocols. Total P was extracted from soils with 1N HCl after ignition at 550 °C (Aspila et al. 1976) and determined by using molybdenum blue and ascorbic acid as reducing agents (Parsons et al. 1984). For N mineralization rates, intact soil

samples were sampled at 10-cm intervals to 40 cm depth with a glass tube (2.5 cm diameter and 10 cm length) inserted within a soil probe. N mineralization rates were based on changes of inorganic N concentrations in intact soils incubated at 25 °C (Chen 1996).

Sedimentation rates were determined with 15.2 cm diameter polyvinyl chloride tubes driven to a depth of 60 cm and sectioned at 2 cm intervals. One core was taken at each of four sites in June 1994. Soil samples were dried at 60 °C to constant mass and weighed for dry bulk density. Concentrations of organic matter, total N, and total P were determined on each section as described above. Organic matter (% ash free dry weight, AFDW) was determined by combusting each sample at 400 °C (Davies 1974). Vertical sediment accretion was determined at S1 and S3 based on depth distribution of ^{210}Pb using sample preparation and dating techniques described by Lynch et al. (1989). Each 2 cm section was counted in a Canberra silicon barrier detector to determine total ^{210}Pb activity. Excess ^{210}Pb activity was determined by subtracting supported ^{210}Pb, as determined by the visual inspection of constant ^{210}Pb activity in the deeper sections of the core, from total ^{210}Pb activity.

Model description

Soil organic matter submodel

A mangrove soil nutrient model (NUMAN) was adapted from a mechanistic and process-based model, SEMIDEC (Morris & Bowden 1986), which simulates the vertical distribution of organic matter, N, and P concentrations, as well as rates of mineralization in marsh sediments. Models using multiple compartments of soil organic matter have been used for terrestrial forests (LINKAGE, Pastor & Post 1986; VEGIE, Aber et al. 1991), grasslands (CENTURY, Parton et al. 1987; Parton et al. 1988) and marshes (Gardner 1990). Two pools of soil organic matter in a marsh are distinguished in the SEMIDEC model. One is the labile organic matter (LOM), with relatively rapid decay, which is analogous to the 'active' fraction of soil organic matter in the CENTURY model (Parton et al. 1987). The other pool is refractory organic matter (ROM), with slower decay, which is conceptually similar to the 'passive' fraction of soil organic matter in the CENTURY model.

A unique characteristic of the SEMIDEC model compared to other soil organic models is the calculation of the vertical profile of organic matter and nutrients. The SEMIDEC uses a life-history approach to describe the dynamics of soil organic matter and treats soil horizons as year-class cohorts, which are modified by root production and decomposition of organic matter

over time as they are buried. A successful feature of the SEMIDEC model is the simulation of diagenesis for a single year cohort of sediment within a specific unit surface area, including calculations of organic matter, N and P contents in the year-class cohort. The input rates of organic and inorganic matter to a sediment cohort are assumed to be constant over time, however, these rates can be a function of time for other applications. The model uses a one year time step.

Our NUMAN model adapted the SEMIDEC approach, with modifications to include some of the biogeochemical processes that are unique to coastal forested wetlands including litter production and wood decomposition. Litter fall can be the major input of organic matter to the soil surface. Annual litter production including leaf litter and twigs (LP, Mg ha^{-1} yr^{-1}) is expressed as a direct function of forest basal area (BA, m^2/ha):

$$LP = 1.33 + 0.292BA. \tag{1}$$

The above equation was obtained by fitting a regression to data collected from 17 mangrove stands in Florida, Puerto Rico and Mexico ($R^2 = 0.6$, $P < 0.0001$; data from Pool et al. 1975; Pool et al. 1977; Heald et al. 1979; Twilley et al. 1986; Day et al. 1987). Besides litter fall, dead trees also contribute organic matter to the forest floor (Robertson & Daniel 1989; Gong & Ong 1990). Not all of these sources contribute organic matter to the soil, some of them are exported by tides and runoff, or consumed by animals (Heald 1969; Boto & Bunt 1981; Twilley 1985). The net accumulation of litter into mangrove soil surface is calculated as:

$$NLP = f_l LP(1.0 - k_e); \tag{2}$$
$$NTP = (1.0 - f_l)LP(1.0 - k_e); \tag{3}$$
$$NWP = k_m B(1.0 - k_e); \tag{4}$$

where NLP, NTP, NWP are annual net accumulation of leaf litter, twigs, and dead wood in mangrove soil surface, respectively. LP is expressed as g cm^{-2} yr^{-1}, f_l is a ratio of leaf litter to total litter, and other parts of litter were treated as twigs. k_e, the rate of litter export, is a site-specific constant related to loss of standing litter, which is a function of hydrology, topography, and the activity and frequency of consumers (Twilley et al. 1997). k_m (yr^{-1}) is the turnover rate of wood biomass and B is above ground biomass (g/cm^2).

Net deposition of leaf litter is assumed to be partitioned directly into two pools corresponding to labile and refractory soil organic matter, which is based on the lignin content (c_0) of leaf litter. The lignin fraction of leaf litter is incorporated into the refractory pool, while the remainder becomes part of the labile pool. The compartments of standing dead wood and twigs have

a specific decay constant, k_w and k_t, respectively. Decomposition of dead wood and twig litter in the surface cohort are separated between microbial respiration and transfer to the ROM pool in the soil. The first stage of decay for both dead wood and twig litter is respiration that represents a mass loss of 45% (f_2), as in the CENTURY model for decomposition of structural organic matter. The contribution of above ground litter to the cohort initially is calculated as:

$$LOM(0) = NLP(1.0 - c_0)(1.0 - c_1); \tag{5}$$

$$ROM(0) = \{c_0\,NLP + (1.0 - f_2)[k_t NTP + k_w NWP]\}(1.0 - c_1); \tag{6}$$

where c_1 is ash content of litter.

The distribution of mangrove roots is an exponential function with depth (Komiyama et al. 1989) as follows:

$$R = R_0 exp(-eD); \tag{7}$$

where R is root mass (g/cm^2) at depth D (cm), R_0 is root mass at the surface (g/cm^2), and e is the attenuation rate (cm^{-1}) of root mass with increasing depth (D) from the surface. Root biomass within a soil cohort was calculated as in the SEMIDEC model:

$$R(t) = R_0 \int_{D_b}^{D_t} exp(-eD)dD = R_0[exp(-eD_b) - exp(-eD_t)]/(-e); \tag{8}$$

where D_b and D_t are the upper and lower depths (cm) of the soil cohort, respectively. Lacking direct information on root biomass for our study sites, we used the following turnover rates to estimate annual fine root production (FRP) (g cm^{-2} yr^{-1}) and large root production (LRP) (g cm^{-2} yr^{-1}) in the soil cohort, respectively:

$$FRP(t) = k_r R(t); \tag{9}$$

$$LRP(t) = k_m R(t); \tag{10}$$

where k_r is turnover rate of fine roots. The turnover rate of main roots is estimated using the rate of above ground wood production (k_m). Upon their death, roots also contribute to pools of LOM and ROM in the soil. The mass of LOM in a soil cohort is based on organic matter input and decomposition in each annual cohort of soil as modified from Morris and Bowden (1986):

$$LOM(t + 1) = LOM(t) - kLOM(t) + [(1.0 - fc_1)FRP(t) + (1.0 - fc_2)LRP(t)](1.0 - c_1) + ROM(t)k_c\,(1.0 - f_2); \tag{11}$$

where k is the decay constant of LOM, fc_1 and fc_2 are fractions of fine roots and large roots that are ROM, respectively. Since decomposition rates of

LOM in above and below ground components of the soil can differ significantly, the NUMAN model modifies the SEMIDEC model by specifying k as either k_a for the decomposition of LOM from t = 0 to 1 or k_b for the decomposition of LOM from t > 1. k_c is the decay constant of ROM.

Inputs of ROM include the refractory fraction of roots and residue from the decomposition of LOM. This pool of ROM decays at a slow rate described by the equation:

$$ROM(t+1) = ROM(t) - k_c ROM(t) + [fc_1 FRP(t) + fc_2 LRP(t)]$$
$$(1.0 - c_1) + kLOM(t)f_3; \tag{12}$$

where f_3 is a proportion of decomposing LOM that enters ROM. Our NUMAN model adapted the CENTURY approach, instead of SEMIDEC, to allow for a flow of organic matter between ROM and LOM, which is indicated in equations (11) and (12). Total organic matter (TOM) in a soil cohort is equal to the sum of these two organic pools plus root organic matter expressed as:

$$TOM(t) = LOM(t) + ROM(t) + R(t)(1.0 - c_1). \tag{13}$$

Inputs of inorganic material to the soil surface include allochthonous inorganic matter and release of minerals from decomposing litter. We assumed that root uptake of inorganic matter is restricted to the top layer of soil, because this is where most of the fine absorbing roots in mangroves soils are found (Clough 1992). The model also assumed that the uptake of inorganic matter for root growth is balanced by release of inorganic matter from dead roots in steady state. Therefore, the amount of inorganic matter within each soil cohort under the surface cohort was assumed constant with depth. The amount of inorganic matter in the surface cohort (W_i) is calculated as:

$$W_i(0) = S_i - c_1(LP + k_m B); \tag{14}$$

where S_i is the annual deposition of mineral sediment (g cm^{-2} yr^{-1}) on the surface including allochthonous input and release from surface litter.

The volume of a soil cohort (V) is expressed as:

$$V(t) = [LOM(t) + ROM(t) + R(t)]/b_o + W_i(t)/b_i; \tag{15}$$

where b_o and b_i are the bulk density of organic matter and inorganic material (g/cm^3) within the soil cohort, respectively. For organic soils, the inorganic term in the above equation (15) is eliminated in the SEMIDEC model. Each

soil cohort in the model represents 1 yr of organic and inorganic matter accumulation per unit area (cm^2) of soil. The volume of a soil cohort is its vertical height (cm), therefore

$$D_b = D_t + V(t); \tag{16}$$

where D_b was solved numerically corresponding to the new cohort depth based on the volume of organic and inorganic matter in that cohort (for a full description of these calculations see Morris & Bowden 1986). Then this new depth was used to calculate root biomass within the soil cohort. The overall bulk density (BD, g/cm^3) of that soil cohort is the sum of LOM and ROM, root biomass and inorganic material divided by height of the cohort using:

$$BD(t) = (LOM(t) + ROM(t) + R(t) + W_i(t))/(D_b - D_t). \tag{17}$$

The SEMIDEC model simulates AFDW concentrations; and we added simulations of bulk density in the NUMAN model. This allowed us to estimate pools of organic matter (g/cm^3) with depth in mangrove soils and compare those simulated concentrations to observed pools of organic matter. Notice that this model does not account for the effect of compaction on soil formation, given the shallow depths that are simulated (to 60 cm depth) in this study.

Soil nitrogen and phosphorus submodel

Two organic N pools are distinguished as labile and refractory N analogous to those used for the organic matter submodel. The total input of N into mangrove wetlands is from atmospheric deposition, N fixation and tidal water exchange (Alongi et al. 1992). The model assumes a total N input (S_n, $gN\ cm^{-2}\ yr^{-1}$) without distinguishing the relative inputs from each source because of a lack of information on each process (Pelegri et al. 1997; Pelegri & Twilley 1998). N cycling in mangrove wetlands is also influenced by processes associated with litter decomposition. Therefore the annual input of N in surface cohort of mangrove soil is assumed as:

$$N_l(0) = (1.0 - fn_1)c_2NLP + (1.0 - fn_2)S_n; \tag{18}$$
$$N_r(0) = fn_1c_2NLP + fn_2S_n + (1.0 - f_2)c_3(k_tNTP + k_wNWP); \tag{19}$$

where respectively, N_l and N_r are labile and refractory organic N; fn_1 and fn_2 are refractory fractions of N from leaf litter and allochthonous inputs; c_2 and c_3 are N concentrations of leaf litter and residual litter.

Following an assumption in the SEMIDEC model, NUMAN calculates N mineralization as proportional to the amount of labile organic N. However,

field studies of N mineralization in mangroves along the Shark River estuary indicated that this process is also influenced by the availability of total P in the soil (Chen 1996). We modified the N mineralization equation in SEMIDEC by multiplying it with a P factor as follows:

$$N_{min}(t) = mN_l(t)P(t-1); \tag{20}$$

where $N_{min}(t)$ is the gross mineralization rate (gN cm^{-2} yr^{-1}). The coefficient m is the specific mineralization rate of labile N, which takes into account the effect of P in a cohort (equation 24 and 25) on N mineralization. Additional N in each cohort is from litter root production using equations from the organic matter submodel. N loss from mangrove soil occurs as a result of plant uptake, immobilization, leaching, ammonia volatilization, and denitrification. The model calculated N loss as a function of gross N mineralization from the soluble N pool, but did not trace the specific processes contributing to N loss:

$$N_l(t+1) = N_l(t) + (1.0 - fn_1)c_4(FRP + LRP) - k_n r N_{min}(t-1); \tag{21}$$
$$N_r(t+1) = N_r(t) + fn_1 c_4(FRP + LRP); \tag{22}$$

where c_4 is N concentration of roots. The coefficients of r and k_n are defined in SEMIDEC as residence time (yr) and specific loss rate (yr^{-1}) of soluble N. Total amount of N in a soil cohort (TN) is calculated as

$$TN(t) = N_l(t) + N_r(t) + c_4 R(t). \tag{23}$$

Inputs of P into mangrove soils include organic P from decomposing litter and allochthonous P deposition on the soil surface. Based on an approach of the SEMIDEC model, the NUMAN model calculates P loss as proportional to the mineralization rate of N:

$$P(0) = S_p + c_5(NLP + k_t NTP + k_w NWP); \tag{24}$$
$$P(t+1) = P(t) + c_5(FRP + LRP) - k_n r N_{min}(t+l)/f_4; \tag{25}$$

where S_p is the annual deposition of allochthonous P (gP cm^{-2} yr^{-1}) on the soil surface, c_5 is the concentration of P in litter. The ratio of P loss relative to the rate of N mineralization is f_4.

Model parameterization and calibration

Literature values

Decay of LOM in the NUMAN model occurs in the surface and sub-surface strata of mangrove soils. The decay constant of leaf litter from experiments using litter bags was used to estimate the decomposition rate of LOM at the soil surface, k_a. The average decay constant of *Rhizophora mangle* and *Avicennia germinans* leaves was 0.9 yr^{-1} in a mangrove wetland of southwest Florida using 1 mm mesh litter bags (Twilley et al. 1986). The decomposition rate of LOM under the surface sediment, k_b, was estimated from a mangrove root decomposition experiment using bags buried in wetland soils (van der Valk & Attiwill 1984). There are only a few measurements of wood decomposition in mangrove wetlands, and results show that decay constants for wood and twigs are 0.083 and 0.276 yr^{-1}, respectively (Robertson & Daniel 1989).

The turnover rate of wood (k_m) was calculated as an average value for the four mangrove sites based on the relationship between woody production and above ground biomass, similar to the assumption in the forest model by Aber et al. (1991). The quantity and productivity of below ground biomass of mangrove wetlands is poorly understood. Two forests in Puerto Rico and Panama dominated by *Rhizophora* have an average ratio of below ground to above ground biomass of 0.74 (Golley et al. 1962; Golley 1975), which was used to calculate below ground biomass for this study. Roots were assumed to be restricted to depth of 150 cm at all four sites in our study.

Parameters in the model including fc_1, fc_2, k_r and k_e are unknown from the literature on mangrove ecology. We assumed that the fraction of fine and large roots that contributed to the pool of ROM was similar to the fraction for leaf litter. A root decomposition experiment demonstrated that the weight loss was higher for main roots than fibrous roots (van der Valk & Attiwill 1984), thus fc_1 was set greater than fc_2 ($fc_1 = 0.25$ and $fc_2 = 0.20$). We used the turnover rate of litter production to above ground biomass (0.05 to 0.15) as an initial estimate of k_r. A value of 0.4 was used for k_e in the initial simulations based on organic matter export in a well-developed *Rhizophora mangle* forest in the North River, near the Shark River estuary (Heald 1969).

Field studies

Two way ANOVA showed that there were significant effects of site on total soil C, N and P in concentration (per unit dry weight) and mass (per unit volume) (Table 3). Total C and N concentrations showed a gradient with an increase from S1 to S6, but values of total C and N per unit volume were higher in S1 and S6 than S3 and S4. In contrast, both total P concentrations
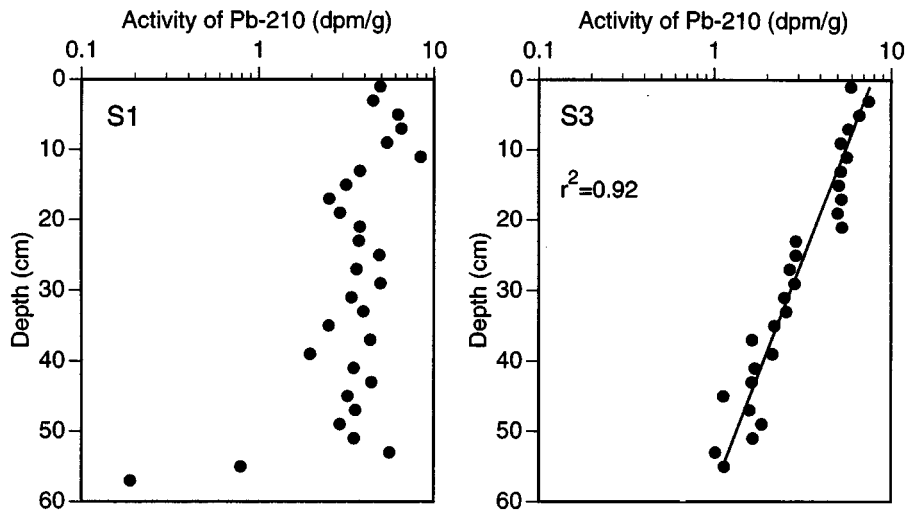
Figure 1. Excess ^{210}Pb activity for the Shark River estuary mangroves, the Everglades National Park.

and mass decreased from S1 and S3 to S6. Generally, the concentrations of C, N and P decreased slightly with depth, however, the effects of depth on these nutrient concentrations were less than that of site (Table 3). Average concentrations of organic matter (% AFDW) to a depth of 60 cm increased from S1 to S6 with values of 30%, 45%, 62% and 82% at S1, S3, S4 and S6, respectively. In contrast to AFDW, bulk density decreased from S1 to S6 with a value of 0.44, 0.22, 0.19 and 0.14 g/cm^3 as a result of increased organic matter content.

The distribution of excess ^{210}Pb activity in a core at S3 was a good fit with depth using an exponential decay model ($R^2 = 0.92$), in contrast to the core at S1 that did not fit the model (Figure 1). The use of ^{210}Pb radionuclides in the measure of accretion rate depends on the assumption of a constant sedimentation rate through time. However, the relative constant concentration of excess ^{210}Pb to a depth of 50 cm in S1 suggests that the sediments were disturbed. The accretion rate for S3 was 0.89 cm/yr according to calculation from a constant activity model. The rate of mineral sediment accumulation (S_i) for S3 was 0.107 $g\ cm^{-2}\ yr^{-1}$, based on a product of the average dry bulk density (g/cm^3), average mineral concentration to the depth of 60 cm, and accretion rate (cm/yr).

Model tuning and sensitivity analyses

Since there is a lack of specific information about N and P biogeochemical processes in mangrove soils, a model tuning procedure was used to adjust

Table 1. Definition and values of parameters used in the NUMAN model.

Para-meters	Definition	Unit	Values	Source
B	Total aboveground biomass	g/cm^2		Table 2
b_o	Bulk density of organic matter	g/cm^3	0.1154	This study
c_0	Lignin content in leaf litter	g/g	0.15	Benner et al. 1990
c_1	Ash concentration in litter	g/g	0.10	Benner et al. 1990
c_2	N concentration in litter	g/g	0.01	Stanford 1976
c_3	N concentration in residual litter	g/g	0.01	Estimated
c_4	N concentration in root	g/g	0.005	Stanford 1976
c_5	P concentration in litter	g/g	0.0002	Stanford 1976
e	A distribution parameter for root biomass	cm^{-1}	0.04	Komiyama et al. 1987
f_1	Ratio of litter leaves to total litter	g/g	0.70	Pool et al. 1975, Twilley et al. 1986
f_2	Proportion of microbial respiration during decomposition	g/g	0.45	Parton et al. 1987
f_3	Proportion of labile organic matter flowing into refractory organic matter after decomposition	g/g	0.004	Parton et al. 1987
f_4	Ratio of N mineralization to P loss	g/g	12.0	Morris & Bowden 1986
fc_1	Fraction of fine root that is refractory	g/g	0.25	Estimated
fc_2	Fraction of large root that is refractory	g/g	0.2	Estimated
fn_1	Fraction of N in litter that is refractory	g/g	0.45	Morris & Bowden 1986
fn_2	Fraction of N from allochthonous source that is refractory	g/g	0.6	Estimated
k_a	Decay constant for labile organic matter on the surface	yr^{-1}	0.90	Twilley et al. 1986
k_b	Decay constant for labile organic matter below the surface	yr^{-1}	0.256	van der Valk & Attiwill 1984
k_c	Decay constant for refractory organic matter	yr^{-1}	0.001	Similar to Parton et al. 1987
k_e	Litter export rate	yr^{-1}		Table 2
k_m	Turnover rate of wood	yr^{-1}	0.0425	Chen 1996
k_n	Specific loss rate of soluble N	yr^{-1}	40.0	Estimated
k_r	Turnover rate of fine roots	yr^{-1}	0.10	Estimated
k_t	Decay constant of litter twigs	yr^{-1}	0.276	Robertson & Daniel 1989
k_w	Decay constant of dead wood	yr^{-1}	0.083	Robertson & Daniel 1989
LP	Litter production	$g\,cm^{-2}\,yr^{-1}$		Table 2
m	Specific mineralization rate of labile N taking account P availability in cohort	$cm^2\,g^{-1}\,yr^{-1}$	5000.0	Estimated
r	Residence time of soluble N in cohort	yr	0.0025	Morris & Bowden 1986
R_0	Total root biomass at the surface	g/cm^2		Table 2
S_i	Annual deposition of mineral sediment	$g\,cm^{-2}\,yr^{-1}$		Table 2
S_n	Annual allochthonous deposition of N	$g\,cm^{-2}\,yr^{-1}$		Table 2
S_p	Annual allochthonous deposition of P	$g\,cm^{-2}\,yr^{-1}$		Table 2

Table 2. Site specific parameters for simulations of the NUMAN model.

Parameter	S1	S3	S4	S6	Methods and source
Basal area (m^2/ha)	40.36	39.67	20.72	19.61	Field survey, Chen 1996
Aboveground biomass (g/cm^2)	2.5	2.5	1.27	0.79	Allometric method, Chen 1996
Belowground biomass (g/cm^2)	1.85	1.85	0.94	0.58	Ratio of below/aboveground biomass
R$_0$ (g/cm^2)	7.4×10^{-2}	7.4×10^{-2}	3.7×10^{-2}	2.3×10^{-2}	Allometric method
LP (g cm^{-2} yr^{-1})	0.131	0.129	0.074	0.071	Regression method
k$_e$ (yr^{-1})	NA	0.4	0.2	0.2	Best estimate
S$_i$ (g cm^{-2} yr^{-1})	NA	1.07×10^{-1}	3.2×10^{-2}	1.5×10^{-2}	Best estimate
S$_n$ (g cm^{-2} yr^{-1})	NA	1.3×10^{-3}	2.0×10^{-4}	0	Best estimate
S$_p$ (g cm^{-2} yr^{-1})	NA	1.9×10^{-4}	4.0×10^{-5}	8.0×10^{-6}	Best estimate

Table 3. Soil C, N and P in mangrove forests along the Shark River estuary. Values are expressed as mean of three stations within 0–40 cm depth in three repeated measurements per site. Summary of F statistics from two way ANOVA of site and depth effects on soil C, N and P. Statistical tests were conducted using mean value of three repeated measurements in a station.

		C		N		P		Atomic	Atomic	Atomic
		(%)	(mg/cm^3)	(%)	(mg/cm^3)	(%)	(mg/cm^3)	C:N	N:P	C:P
Mean value by site										
S1		14.31	51.4	0.70	2.51	0.105	0.38	24.7	14.8	356
S3		22.19	39.3	1.15	2.03	0.118	0.21	22.9	21.6	488
S4		32.50	46.1	1.55	2.19	0.088	0.13	24.7	39.5	969
S6		43.34	50.3	2.33	2.70	0.057	0.07	21.8	102.3	2224
F-statistics										
Sources	df									
Site	3,32	2317.9***	22.2***	1637.4***	21.5***	205.0***	500.4***	19.5***	371.9***	375.2***
Depth	3,32	24.2***	ns	21.6***	3.1*	9.5***	3.5*	ns	14.0***	15.3***
Site*Depth	9,32	6.3***	ns	7.8***	ns	9.3***	3.7**	3.6**	21.8***	21.6***

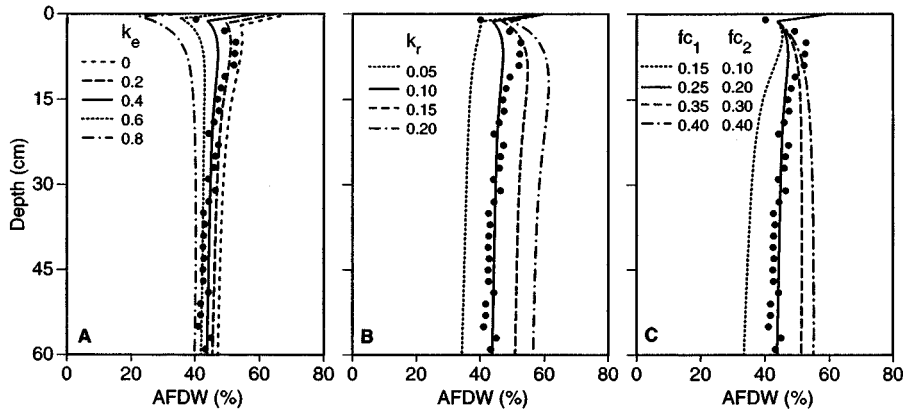* $P \leq 0.05$, ** $P \leq 0.01$, or *** $P \leq 0.001$, ns = no significance.

Figure 2. Sensitivity analysis of model input parameters. Dots represent the observed results. A) Litter export (k_e); B) Fine root turnover rate (k_r); C) Fraction of organic matter which is in refractory organic matter in fine roots (fc_1) and main roots (fc_2). Parameters $k_e = 0.4$, $k_r = 0.10$, $fc_1 = 0.25$ and $fc_2 = 0.2$ were set if they were not tested parameters.

several parameters related to the N and P submodels which include k_n, m, S_n and S_p. And other parameters, such as r and f_4 are from the SEMIDEC model. The parameters fc_1, fc_2, k_r and k_e were also estimated using a model-tuning procedure (Parton et al. 1987), where the parameters were systematically adjusted to accomplish a best fit of measured and simulated profiles of organic matter content and bulk density. Observed profiles of organic matter and bulk density for S3 were chosen to tune these input parameters, because a reasonable fit of excess ^{210}Pb profile to the exponential decay model was observed (Figure 1). Sensitivity analyses of these input parameters were conducted by varying one parameter at a time while keeping the other parameters constant.

The accumulation of mineral sediments calculated from ^{210}Pb measurements was used as a parameter of inorganic inputs (S_i) for S3. Having a fixed estimate of this parameter, a series of simulations were conducted to test the sensitivity of litter export, root turnover, and organic matter quality on organic matter accumulation in mangroves soils (Figure 2). An increase in the loss of litter from the surface of mangrove soils (k_e) causes a significant decrease in organic matter content at the top 10 cm of soil (Figure 2A). However, there was only a 10% change in concentration of organic matter at 30 cm by varying litter export (k_e) from 0 to 0.8 among simulations. After the initial decrease, concentration of organic matter increased with depth when the export was higher, however, organic matter content decreased with depth when export was lower. By fitting with an observed profile of organic matter concentrations in S3, the model suggests that the export coefficient (k_e) in this site is about 0.4.

Root production in the model had more influence on organic matter content than litter export as indicated by an increase of 20% AFDW below 10 cm depth when the fine root turnover rate, k_r, increased from 0.05 to 0.2 (Figure 2B). Changes in k_r had minor influence on the concentration of organic matter in the surface sediment, in contrast to changes in k_e. Changes in the refractory fraction of root organic matter also had significant effects on the profiles of organic matter content (Figure 2C). The organic matter content was 35% at 60 cm when the refractory fraction was low ($fc_1 = 0.15$ and $fc_2 = 0.1$); however, concentrations increased to 55% when refractory fraction was higher (fc_1 and $fc_2 = 0.4$). After a series of model runs, a reasonable combination of input parameters (k_r, fc_1 and fc_2) was estimated for the study sites (Tables 1 and 2).

Model calibration

The model was calibrated by simulating soil profiles of organic matter and nutrients at four mangrove sites along the Shark River estuary using values of forest biomass at each respective site as initial conditions. The model assumed that forest structure at all sites was in steady state and thus no changes in biomass and basal area were calculated during the simulations. The NUMAN model also assumed that the export of litter (parameter k_e) and allochthonous mineral input (parameter S_i) in the four study sites decreased with distance from the mouth of the estuary (Table 2). The profile of excess ^{210}Pb activity (Figure 1A) and bulk density (Figure 3) demonstrate that the mangrove soil in S1 has been highly disturbed. Accordingly, the vertical bulk density at this site also varies from 0.3 to 0.6 g/cm^3. Vertical profiles of organic matter and bulk density in soils at S3, S4 and S6 exhibited less differences with depth compared with those at S1 (Figure 3). Simulations of organic matter content in S1 fit the mean of observed results, but simulated bulk densities were significantly different from observed results. These variations in bulk density with depth clearly invalidate the steady state assumption for sediment input rate for S1. Therefore, the major comparisons of simulated and observed results were conducted at S3, S4 and S6 where disturbance is less evident.

Time periods represented by simulations of 60 cm depth profiles for S3, S4 and S6 were 95, 230 and 370 yrs, respectively. The differences between simulated and observed concentrations of AFDW were within 8% of observed concentrations in S3, S4 and S6 below 5 cm (Figure 3). Generally, the model predicted a quick decrease of AFDW at the surface, because of the rapid decomposition of LOM. The predicted depth of rapid organic matter decomposition varied among sites. Simulations showed that AFDW at S4 and S6 increased slowly below the rapid decomposition layer, which was an excellent fit to the observed profile below 8 cm. In contrast, the model did not predict an increase in AFDW below the rapid decomposition layer at S3, but showed
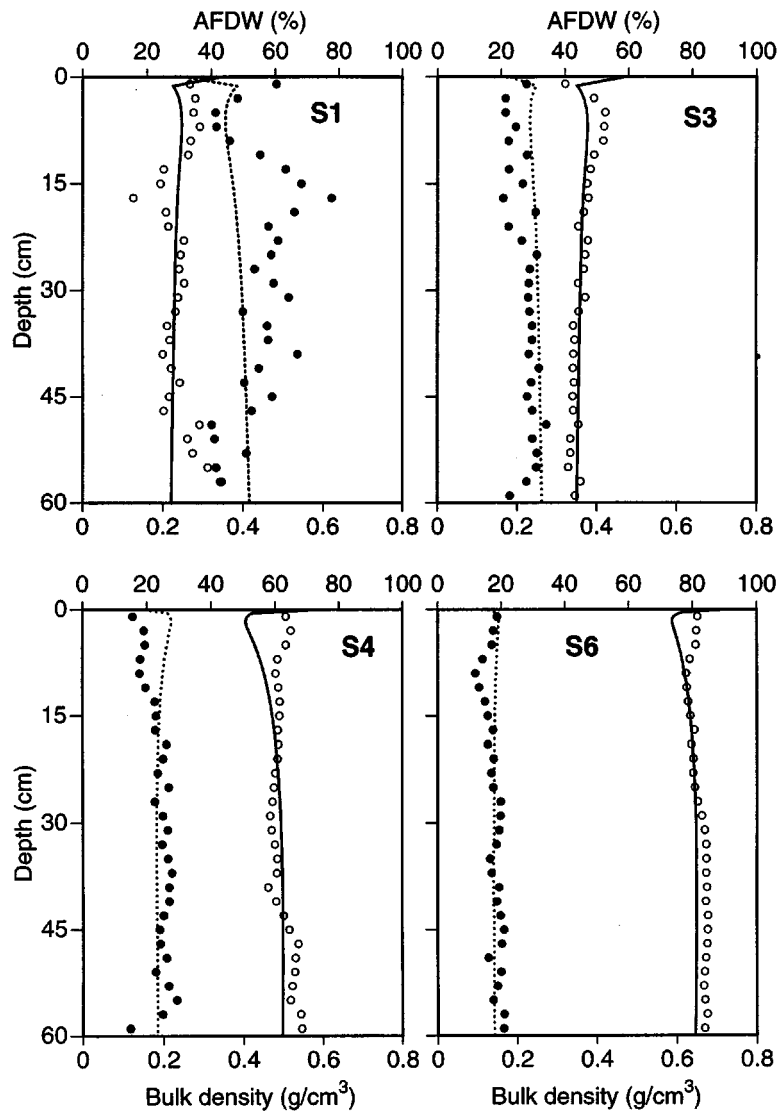
Figure 3. Comparison of observed concentrations of organic matter (AFDW%) (circle) with simulated concentrations (solid line) and observed bulk density (solid dot) with simulated bulk density (dash line) in mangrove soils for the downstream (S1 and S3), intermediate (S4) and upstream (S6) sites along the Shark River estuary.

a relatively constant concentration with depth. The discrepancies in AFDW profiles among the downstream (S3), intermediate (S4) and upstream (S6) sites were due to higher deposition rates of allochthonous mineral sediment at the sites near the mouth of the estuary. The simulated profiles of bulk density showed a decreasing trend with increased distance from the mouth of the

estuary, and simulated bulk densities were a reasonable fit to observed values in S3, S4 and S6.

The simulated N concentrations were within the range of concentrations of observed profiles at S3, S4 and S6 (Figure 4). The model predicted a slight decrease in N concentrations following an initial increase in surface soils in the three sites, which fits well with the observed N profiles. Differences between simulated and observed N concentrations in S3 and S4 were within 16% of the observed values except at the soil surface. The greatest difference between simulated and observed N concentrations was observed at 25 cm depth in S6 at 30%. However, simulated values at this depth were within the range of observed values using two different sampling methods.

Daily rates of net N mineralization at each mangrove site were averaged from field measurements on three sampling dates, and extrapolated to an annual rate for comparison with simulated gross mineralization rates (Figure 5). Note that the observed N mineralization rates were representative of 10 cm sections (to a depth of 40 cm), however, simulated values were calculated for each soil cohort section. Both the simulated and observed N mineralization rates in each study site decreased quickly with depth, except for the observed values in S1. Simulated rates of N mineralization were higher than observed values, which may be an artifact due to difference in field methods and operational definitions of this process within NUMAN. Laboratory incubations of mangrove soil in this study provided an index of net N mineralization during the incubation period, including microbial N consumption during organic matter mineralization. Therefore, it is reasonable that estimates of N mineralization by the model were higher than net mineralization rates measured in laboratory incubations. The gross N mineralization rates integrated to a depth of 0–40 cm calculated by NUMAN increased from the oligohaline to marine sites along the Shark River estuary with values of 2.6 (S6), 5.1 (S4) and 13.3 (S3) $mgN \, cm^{-2} \, yr^{-1}$.

Parameter S_p, the annual input of allogenic inorganic and organic P through deposition of sediment particles or adsorption from flooding waters, was adjusted to fit the P profile for each site (Table 2, Figure 6). Both observed and simulated P concentrations in S3 decreased gradually below an initial increase. Simulated P concentrations increased rapidly in the top 1 cm of soil in S4 and S6, then decreased rapidly with depth. Decreases in P concentrations in the model fit well with the observed P profile, which corresponded with a release of P from organic matter associated with N mineralization.
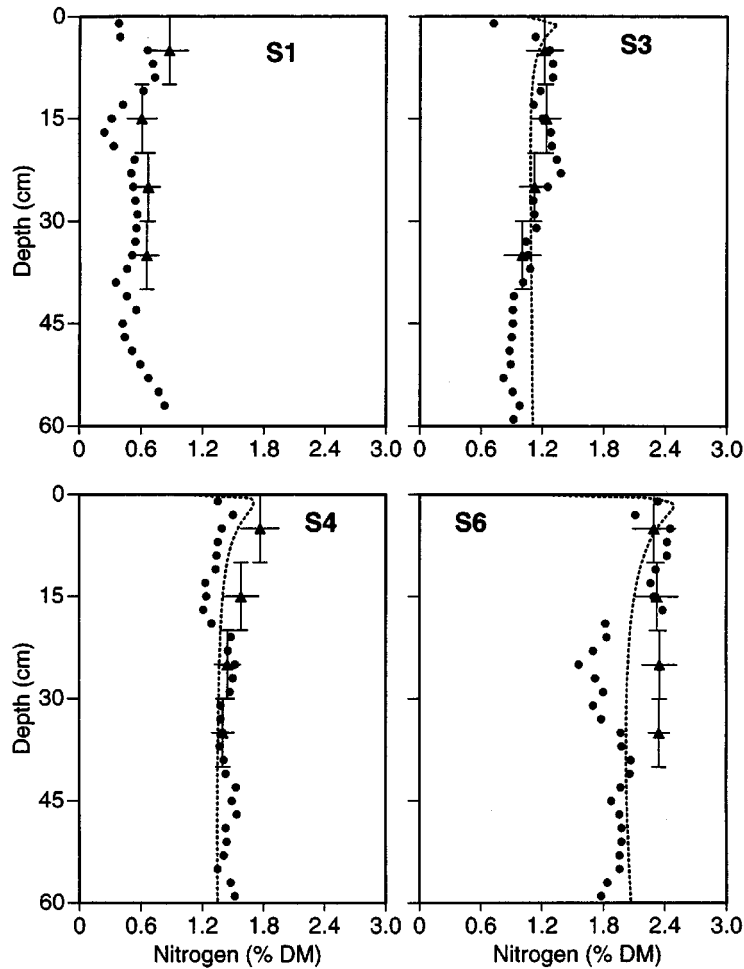
Figure 4. Comparison of observed concentrations (% of dry mass) of nitrogen with simulated concentrations (dashed line) in mangrove soils for the downstream (S1 and S3), intermediate (S4) and upstream (S6) sites along the Shark River estuary. Solid dots represent results from one 15.2 cm diameter core at each site. Triangles represent mean values from 3 stations in 3 repeated samplings. Bar along the x-axis is standard deviation ($n = 9$); bar along the y-axis is interval of integrated sampling depth.

Discussion

One of the objectives of the NUMAN model was to identify those ecological processes that are poorly understood, yet make significant contributions to the biogeochemical properties of a mangrove ecosystem. Mangrove plant production has been recognized as a major component in the formation of mangrove soils and mangrove peat in south Florida, particularly the turnover
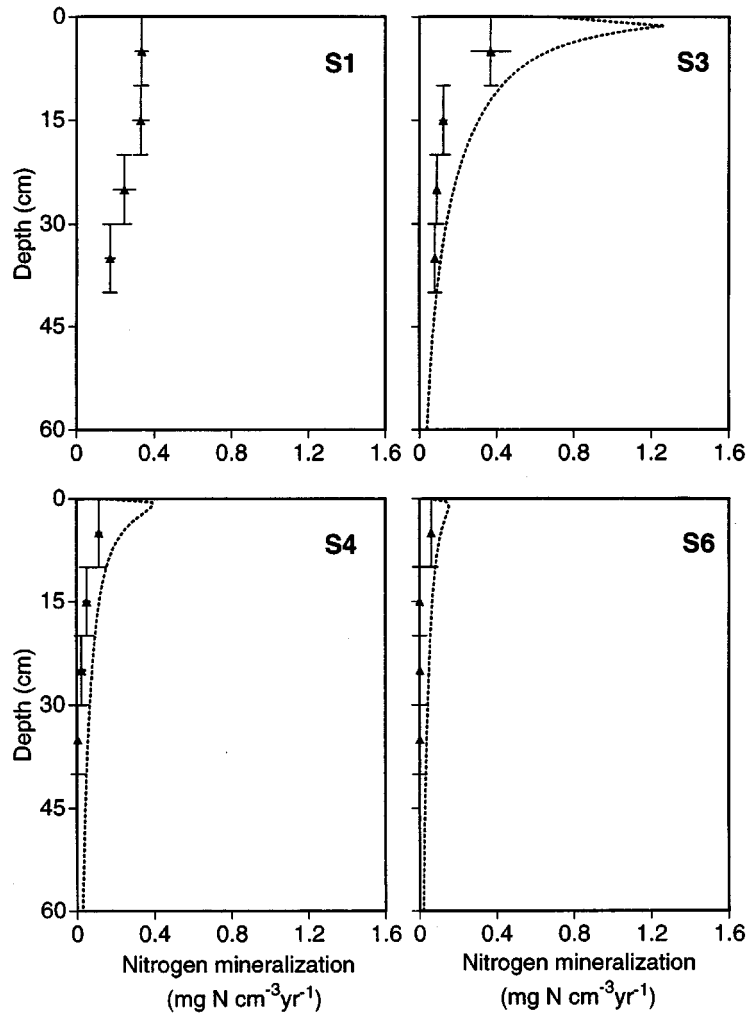
Figure 5. Comparison of observed N mineralization rates with simulated rates (dashed line) in mangrove soils for the downstream (S1 and S3), intermediate (S4) and upstream (S6) sites along the Shark River estuary. See legend of Figure 4 for meaning of symbols.

of mangrove rootlets (Davis 1940; Scholl 1964a, b; Cohen & Spackman 1974). Simulation results of NUMAN suggest that rates of root production, along with the concentration of ROM in dead roots, are critical processes in controlling organic matter accumulation and the vertical distribution of organic matter in mangrove soils. Yet these two variables lack any direct verification in mangrove studies. Variation in rates of root turnover are more important than changes in rates of litter fall export on the organic matter profiles in mangroves soils under 10 cm depth. This conclusion that root
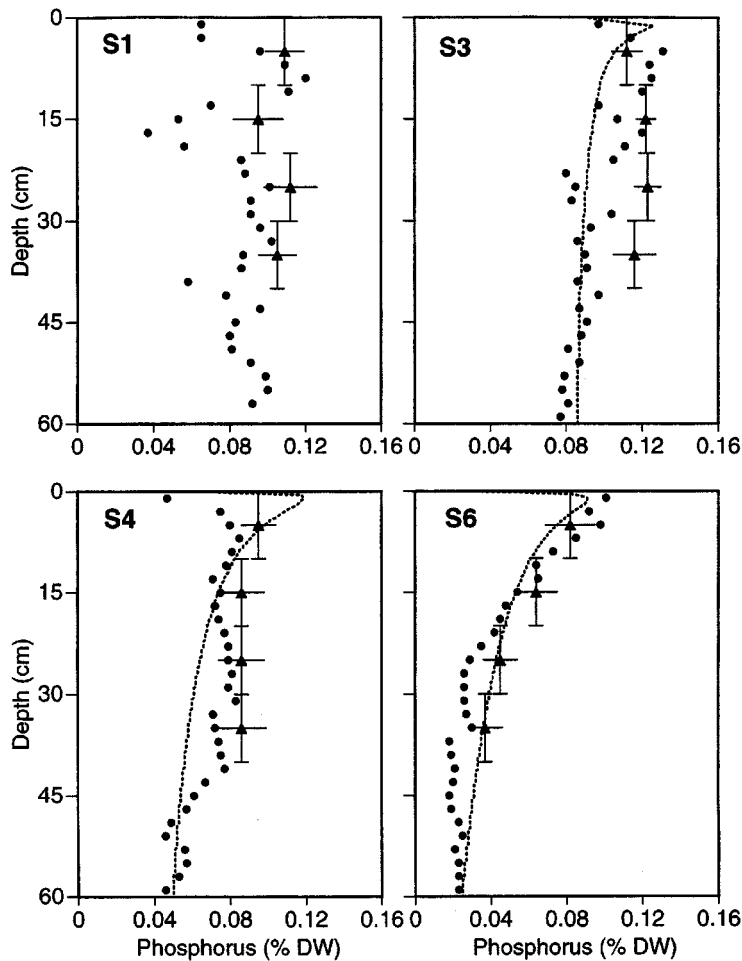
Figure 6. Comparison of observed concentrations of phosphorus (% of dry mass) with simulated concentrations (dashed line) in mangrove soils for the downstream (S1 and S3), intermediate (S4) and upstream (S6) sites along the Shark River estuary. See legend of Figure 4 for description of symbols.

production is more significant to soil formation than litter fall is interesting given the much larger research emphasis on litter dynamics in mangrove wetlands (Twilley et al. 1997). Many of the below ground processes in this version of NUMAN are assumptions based on amount and productivity of above ground biomass (Tables 1 and 2), emphasizing the need for more research in root biomass and production of mangrove forests. Direct measurements of root production in mangrove wetlands are difficult, especially in

identifying dead and live roots, and these model simulations provide one of the first estimates of below ground production and turnover.

Field measurements of soil organic matter showed that concentrations along the Shark River estuary increased dramatically with increased distance from the estuary mouth, while bulk densities decreased. These trends suggest that sedimentation rates decreased along the axis of the estuary. Because data on sedimentation rates are limited, rates of inorganic mineral input simulated by NUMAN were not verified for sites S1, S4 and S6. Instead, we adjusted the amount of inorganic material input among these sites until simulations matched the spatial gradient of soil profiles of bulk density and AFDW from downstream to upstream locations. Adjusted rates were within a reasonable range as compared to previous studies of sediment accumulation among mangrove forests (Lynch et al. 1989), which vary significantly among ecological types of mangroves, ranging from 107 to 1404 $g\,m^{-2}\,yr^{-1}$. Model simulations for S4 using a litter export rate of 20% ($k_e = 0.20$) required an input of 320 $g\,m^{-2}\,yr^{-1}$ of inorganic material to fit the soil profile of bulk density and AFDW at this site. This sedimentation rate is between the measured rate of inorganic sediment accumulation in Rookery Bay basin forest (107–179 $g\,m^{-2}\,yr^{-1}$) and in Estero Pargo fringe mangroves (566 $g\,m^{-2}\,yr^{-1}$) (Lynch 1989). Mineral input in S6 (150 $g\,m^{-2}\,yr^{-1}$) estimated by the model is within the range of a basin forest in Rookery Bay, which receives very little sediment input. The low rate of inorganic sediment input at S6 may be due to low concentrations of suspended sediment from the Shark River Slough, and increased distance from the Gulf of Mexico.

The spatial pattern of P accumulation in mangrove soils simulated by NUMAN follows a similar pattern as inorganic sediments with reduced input rates as distance from the mouth of the estuary increases. Estimates of P accumulation by NUMAN for S3, S4 and S6 were 1.9, 0.4, and 0.08 $g\,m^{-2}\,yr^{-1}$, respectively, consistent with higher P concentrations in mangrove soils at the mouth of Shark River estuary. Comparisons of inorganic and P accumulation in mangrove sediments in a wide range of environmental settings have shown a strong correlation between inorganic sediment and P accumulation (Twilley 1995). These simulations support the hypothesis that sediment resuspension and transport to mangroves at the mouth of Shark River estuary results in higher soil fertility in contrast to the lack of sediment and P loading in the tidal freshwater regions of Shark River Slough (Chen 1996). P accumulation in freshwater soils of the Everglades ranges from 0.11 to 1.14 $g\,m^{-2}\,yr^{-1}$ (Reddy et al. 1993) and 0.10 to 0.66 $g\,m^{-2}\,yr^{-1}$ (Craft & Richardson 1993) depending on distance from agriculture effluent. This range in the Everglades is similar to simulations of the NUMAN model for upper (S6) and intermediate (S4) sites along the Shark River estuary. But the lower estuary site (S3)

has P accumulation rates that are higher than the nutrient enriched sites of the Everglades.

The ability of NUMAN to simulate organic matter diagenesis in mangrove soils was limited by the assumption that ecological processes throughout the 60-cm profile are in steady state. ^{14}C dating techniques revealed that mangroves have developed in the Shark River region over the past 3000 yrs (Scholl 1964a, b). Mangrove rootlets have contributed significantly to the 1–4 m of peat developed during the late Holocene transgression (Davis 1940; Craighead 1971). However, hurricanes, which are one of major large scale and cyclic disturbances of mangroves in south Florida (Lugo & Snedaker 1974), can destroy mangrove biomass and redistribute tremendous amounts of sediment in mangrove wetlands (Smith et al. 1994). These processes can seriously influence model simulations based on steady state assumptions of forest growth and inorganic deposition. Observed soil profiles in S1 exhibited obvious shifts in bulk density and organic matter with depth. These sharp gradients in soil profiles probably reflect different sedimentation rates in this site. Integrating the NUMAN model to simulate soil fertility with FORMAN, which is a gap dynamics model of mangrove forest development (Chen & Twilley 1988), should provide feedback effects of biogeochemical processes and organic productivity in mangrove ecosystems. These models will have to include the role of disturbance in the distribution of resources and reduction in forest production to adequately simulate complex biogeochemical processes in mangrove wetlands.

Acknowledgements

References

Aber JD, Melillo JM, Nadelhoffer KJ, Pastor J & Boone RD (1991) Factors controlling nitrogen cycling and nitrogen saturation in northern temperate forest ecosystems. Ecological Application 1: 303–315

Alongi DM, Boto KG & Robertson AI (1992) Nitrogen and phosphorous cycles. In: Robertson AI & Alongi DM (Eds) Tropical Mangrove Ecosystems (pp 252–292). American Geophysical Union, Washington, DC

Aspila KI, Agemian H & Chau ASY (1976) A semi-automated method for the determination of inorganic, organic and total phosphate in sediments. Analyst 101: 187–197

Benner R, Hatcher PG & Hedges JI (1990) Early diagenesis of mangrove leaves in a tropical estuary: Bulk chemical characterization using solid-state ^{13}C NMR and elemental analyses. Geochimica et Cosmochimica Acta 54: 2003–2013

Boto KG & Bunt JS (1981) Tidal export of particulate organic matter from a northern Australian mangrove system. Estuarine, Coastal and Shelf Science 13: 247–255

Boto KG & Wellington JT (1984) Soil characteristics and nutrient status in a northern Australian mangrove forest. Estuaries 7: 61–69

Chen R (1996) Ecological Analysis and Simulation Models of Landscape Patterns in Mangrove Forest Development and Soil Characteristics Along the Shark River Estuary, Florida. Dissertation, University of Southwestern Louisiana, Lafayette, Louisiana

Chen R & Twilley RR (1998) A gap dynamic model of mangrove forest development along gradients of soil salinity and nutrient resources. Journal of Ecology 86: 37–52.

Clough BF (1992) Primary productivity and growth of mangrove forest. In: Robertson AI & Alongi DM (Eds) Tropical Mangrove Ecosystems (pp 225–249). American Geophysical Union, Washington DC

Cohen AD & Spackman W Jr (1974) The petrology of peats from the Everglades and coastal swamps of southern Florida. In: Gleason PJ (Ed) Environments of South Florida: Present and Past II (pp 233–255). Miami Geology Society, Coral Gables, Florida

Craft CB & Richardson CJ (1993) Peat accretion and phosphorus accumulation along a eutrophication gradient in the northern Everglades. Biogeochemistry 22: 133–156

Craighead FC (1971) The Trees of South Florida. University of Miami Press, Coral Gables, Florida, USA

Davies BE (1974) Loss-on-ignition as an estimate of soil organic matter. Soil Science Society of America Proceedings 38: 150–151

Davis JH Jr (1940) The ecology and geologic role of mangroves in Florida. Carnegie Institute of Washington Publication Number 517: 303–412

Day JW, Conner WH, Ley-Lou F, Day RH & Navarro AM (1987) The productivity and composition of mangrove forests, Laguna de Términos, Mexico. Aquatic Botany 27: 267–284

Duke NC (1992) Mangrove floristics and biogeography. In: Robertson AI & Alongi DM (Eds) Tropical Mangrove Ecosystems (pp 63–100). American Geophysical Union, Washington DC

Gardner LR (1990) Simulation of the diagenesis of carbon, sulfur, and dissolved oxygen in salt marsh sediments. Ecological Monographs 60: 91–111

Golley FB (1975) Mineral Cycling in a Tropical Moist Forest Ecosystem. University of Georgia Press, Athens, Georgia

Golley FB, Odum HT & Wilson R (1962) A synoptic study of the structure and metabolism of a red mangrove forest in southern Puerto Rico in May. Ecology 43: 9–18

Gong WK & Ong JE (1990) Plant biomass and nutrient flux in a managed mangrove forest in Malaysia. Estuarine, Coastal and Shelf Science 31: 519–530

Heald EJ (1969) The Production of Organic Detritus in a South Florida Estuary. Dissertation, University of Miami, Coral Gables, Florida

Heald EJ, Roessler MA & Beardsley GL (1979). Litter production in a southwest Florida black mangrove community. In: Rathburn CB (Ed) Florida Anti-Mosquito Association 50th Meeting (pp 24–32)

Komiyama A, Moriya H & Ogino K (1989) A quantitative analysis of root system of mangrove tree species in Iriomote Island, southern Japan. Galaxea 8: 89–96

Lugo AE & Snedaker SC (1974) The ecology of mangroves. Annual Review of Ecology and Systematics 5: 39–64

Lynch JC (1989) Sedimentation and Nutrient Accumulation in Mangrove Ecosystem of the Gulf of Mexico. M.S. Thesis, University of Southwestern Louisiana, Lafayette, Louisiana

Lynch JC, Meriwether JR, McKee BA, Vera-Herrera F & Twilley RR (1989) Recent accretion in mangrove ecosystem based on ^{137}Cs and ^{210}Pb. Estuaries 12: 284–299

Morris JT & Bowden WB (1986) A mechanistic, numerical model of sedimentation, mineralization, and decomposition for marsh sediments. Soil Science Society of America Journal 50: 96–105

Parkinson RW, DeLaune RD & White JR (1994) Holocene sea-level rise and the fate of mangrove forests within the wider Caribbean region. Journal of Coastal Research 10: 1077–1086

Parsons TR, Maita Y & Lalli CM (1984) A Manual of Chemical and Biological Methods for Seawater Analysis. Pergamon Press, New York

Parton WJ, Schimel DS, Cole CV & Ojima DS (1987) Analysis of factors controlling soil organic matter levels in Great Plains grasslands. Soil Science Society of America Journal 51: 1173–1179

Parton WJ, Stewart JWB & Cole CV (1988) Dynamics of C, N, P and S in grassland soils: a model. Biogeochemistry 5: 109–131

Pastor J & Post WM (1986) Influence of climatic, soil moisture, and succession on forest carbon and nitrogen cycles. Biogeochemistry 2: 3–27

Pelegri SP, Rivera-Monroy VH & Twilley RR. (1997) A comparison of nitrogen fixation (acetylene reduction) among three species of mangrove litter, sediments, and pneumatophores in south Florida, USA. Hydrobiologia 356: 73–79.

Pelegri SP & Twilley RR. (1998) Interactions between nitrogen fixation (acetylene reduction) and leaf litter decomposition of two mangrove species from south Florida, USA: Potential inhibitory effects of phenolics. Marine Biology XX: 000–000.

Pool DJ, Lugo AE & Snedaker SC (1975). Litter production in mangrove forests of southern Florida and Puerto Rico. In: Walsh GE Snedaker SC Teas HJ (Eds) Proceedings of the International Symposium on Biology and Management of Mangroves (pp 213–237). East-West Center, Honolulu, Hawaii

Pool DJ, Snedaker SC & Lugo AE (1977) Structure of mangrove forests in Florida, Puerto Rico, Mexico, and Costa Rica. Biotropica 9: 195–212

Reddy KR, DeLaune RD, DeBusk WF & Koch MS (1993) Long-term nutrient accumulation rates in the Everglades. Soil Science Society of America Journal 57: 1147–1155

Robertson AI & Daniel PA (1989) Decomposition and the annual flux of detritus from fallen timber in tropical mangrove forests. Limnology and Oceanography 34: 640–646

Scholl DW (1964a) Recent sedimentary record in mangrove swamps and rise in sea level over the southwestern coast of Florida, Part I. Marine Geology 1: 344–366

Scholl DW (1964b) Recent sedimentary record in mangrove swamps and rise in sea level over the southwestern coast of Florida, Part II. Marine Geology 2: 343–364

Smith TJ III, Robblee MB, Wanless HR & Doyle TW (1994) Mangroves, hurricanes, and lightning strikes. BioScience 44: 256–262

Stanford RL (1976) Nutrient Cycling in a South Florida Mangrove Ecosystem. M.S. Thesis. University of Florida, Gainesville, Florida

Thom BG (1982) Mangrove ecology – a geomorphological perspective. In: Clough BF (Ed) Mangrove Ecosystems in Australia (pp 3–17). Australian National University Press, Canberra

Twilley RR (1985) The exchange of organic carbon in basin mangrove forests in a southwest Florida estuary. Estuarine, Coastal and Shelf Science 20: 543–557

Twilley RR (1995) Properties of mangrove ecosystems related to the energy signature of coastal environments. In: Hall C (Ed) Maximum Power (pp 43–62). University of Colorado Press, Boulder, Colorado

Twilley RR, Chen R & Hargis T (1992) Carbon sinks in mangroves and their implications to carbon budget of tropical coastal ecosystem. Water, Air, and Soil Pollution 64: 265–288

Twilley RR, Lugo AE & Patterson-Zucca C (1986) Production, standing crop, and decomposition of litter in basin mangrove forests in southwest Florida. Ecology 67: 670–683

Twilley RR, Pozo M, Garcia VH, Rivera-Monroy VH, Zambrano R & Bodero A (1997) Litter dynamics in riverine mangrove forests in the Guayas River estuary, Ecuador. Oecologia 111: 109–122

van der Valk AG & Attiwill PM (1984) Decomposition of leaf and root litter of *Avicennia marina* at Westernport Bay, Victoria, Australia. Aquatic Botany 18: 205–221